Optimal Placement of Wind Turbines in Wind Farm Layout Using Particle Swarm Optimization

Philip Asaah, Lili Hao, and Jing Ji

Abstract—**An optimal geographical location of wind turbines can ensure the optimum total energy output of a wind farm. This study introduces a new solution to the optimization of wind farm layout (WFLO) problem based on a three-step strategy and particle swarm optimization as the main method. The proposed strategy is applied to a certain WFLO to generate highly efficient optimal output power. Three case scenarios are considered to formulate the non-wake and wake effects at various levels. The required wind turbine positions within the wind farm are determined by the particle swarm optimization method. The rule of thumb, which determines the wind turbine spacing, is thoroughly considered. The MATLAB simulation results verify the proposed three-step strategy. Moreover, the results are compared with those of existing research works, and it shows that the proposed optimization strategy yields a better solution in terms of total output power generation and efficiency with a minimized objective function. The efficiencies of the three case studies considered herein increase by 0.65%, 1.95%, and 1.74%, respectively. Finally, the simulation results indicate that the proposed method is robust in WFLO design because it further minimizes the objective function.**

Index Terms—**Jensen model, particle swarm optimization, wake effect, wind farm layout (WFLO), wind turbine.**

I. Introduction

IN recent years, many renewable energies have emerged to support conventional power generation because of the depletion of fossil fuel sources and the increase of electricity demand.

Although wind energy provides clean energy, the generation of higher output energy cannot be obtained because of the wake effect, which can be defined as the reduction in wind speed as it passes through the rotor of a wind turbine (WT); this effect also generates turbulence (usually referred to as wake effect) in turbines. Accordingly, the optimization of wind farm layout (WFLO) becomes more important. An inadequately optimized WFLO would result in decreased output power and increased operation and maintenance costs as well as wear and tear, leading to shorter WT component lifespan [1], [2]. For instance, the increase in turbulence coupled with the variable wind speed considerably impacts the WT, particularly the gearbox lifespan because of fatigue [3], [4]. Therefore, retarding the deterioration rate of the WT caused by turbulence is extremely critical for prolonging its lifespan. It is estimated that the wake effect reduces the wind farm output power by 10%-15% [5]. To reduce the wake effect in a restricted area for optimal energy production and advance the WT design and arrangement, it is critical to consider other factors such as wind farm elevation, wind speed, wind direction, and hub height in the design process.

The wake effect can be managed, if not eliminated, by carefully considering the geographical location and installation position of each WT. The ability to minimize the wake effect in a limited area is one of the key requisites for maximizing the output power of the wind farm. There are problems in the existing optimization strategies for determining the optimal number of WTs and locations of a given wind farm. Directly or indirectly, they reduce the wake effect in a restricted location to a certain extent.

In the wind farm design, the WT layouts either employ the same specifications [6] or use multiple specifications [7] in formulating the WFLO. The use of multiple specifications provides system flexibility and robustness. However, because optimization algorithms have many parameter values, they are easily constrained by the computation complexity. For instance, in [8], the authors proposed a WFLO problem with a continuous selection of WTs and hub heights using Cartesian coordinates and a single-objective genetic algorithm (GA) to improve the total output power. The hub heights were also restrained within a predefined range. In [7], to minimize the cost per unit power in the WFLO with multiple hub heights, a three-dimension greedy algorithm was applied. Moreover, in [6], the area rotation method and definite point selection technique were proposed to determine the optimal dimensions and position of the wind farm. The area rotation method enabled the maximum area of the wind farm to capture the freestream velocity to some extent. In addition to the aforementioned techniques, which had delayed solution convergence, several optimization scenarios were conceived for terrain and non-terrain locations to formulate the wake effect.

System designers highly recommend the use of WTs with the same specifications because of its feasibility and low operation cost. The first WFLO problem formulated to determine the required number and position of WTs in a given location was solved by [9]. The authors optimized the required

Manuscript received: November 10, 2019; accepted: February 24, 2020. Date of CrossCheck: February 24, 2020. Date of online publication: March 9, 2021.

P. Asaah, L. Hao (corresponding author), and J. Ji are with the College of Electrical Engineering and Control Science, Nanjing Tech University, Nanjing 210008, China (e-mail: asaahphilip@yahoo. com; lili_hao@163. com; 708878505@qq.com).

DOI: 10.35833/MPCE.2019.000087

number of WTs for a given parcel of land in three different cases of wind speeds and directions. This was further advanced by [10]. In these studies, the optimization parameter values were slightly modified using GA. The modifications further improved the optimal positions of the WTs. In [11], the authors recommended an increase in the size of wind farm boundaries as that in [9], [10], and [12] from 2 km × 2 km to 2 km × 2.2 km. Three case scenarios were adopted for the analysis. The results showed that the solvement of WFLO problem using micro-siting technique and GA was relatively successful. These optimization methods were constrained by boundaries, and a WT could only be installed at the center of a selected cell. In [13], the geometric pattern-based approach was employed to position the WTs to maximize the total output power of the wind farm and overcome the sub-optimality in the solution space. The implementation of the approach was successful. However, the available wind farm area for the grid-based turbine placement was not efficiently exploited. Again, the highly significant wake effects were not adequately considered.

To increase the movement range of the WTs within a given geographical location, more algorithms have been developed. In [14], for a circular wind farm, a biogeography-based optimization method was employed to position the WTs with a limited rotor diameter and within the boundary to maximize the expected output energy. In situations where numerous parameters are required for optimization, the high correlation complexities always affect the computational efficiency. In [15], a regular wind farm was optimized considering three aspects: placement direction of wind farm, spacing of each pair of WTs, and control strategy of wind farm. An adaptive particle swarm optimization (PSO) [16]-[18] was adopted for the optimization of WT layout to increase the possibility of finding the global optimum. The best tradeoff between energy yields and capital investments is obtained because of the appropriate positioning of the WTs. With all these achievements, the accuracy of the control strategy is only based on the accuracy of the wake model necessary to predict the wind speed at each WT. In [19], a multi-objective function was proposed to minimize the layout cost and maximize the energy output using the PSO algorithm. Despite the successful implementation, the wake effect and discounted cost of the wind farm during the life cycle were not considered. To harvest additional maximum output power, a PSO with multiple adaptive methods was also proposed in [20]. Some restricted zones were used without sufficiently considering the spacing of the WTs.

With the successful implementation of PSO, if additional considerations are made on the layout and the wake effect is regulated with respect to the rule of thumb, an efficient position will be obtained for the optimal output power in any restricted wind farm location. Accordingly, a three-step strategy is proposed to minimize the objective function.

The remainder of this paper is organized as follows. Section II introduces the mathematical modeling of WFLO employed in the study. Section III outlines the three-step strategy for the WFLO. The simulation results of the proposed method are discussed in Section IV, and the conclusions are summarized in Section V.

II. Mathematical Modeling of WFLO

A. Wake Effect Modeling

A WT has two main effects: wind speed reduction and turbulence. This wake effect on the WT is illustrated in Fig. 1. The upstream or freestream wind speed u_o decreases to the downstream wind speed u_i as the wake boundary linearly expands downwards.

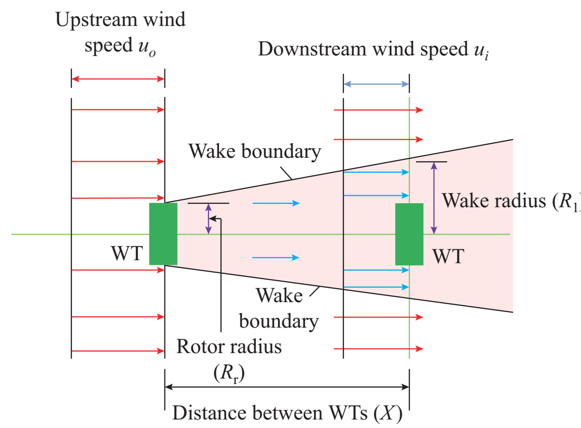

Fig. 1. Schematic diagram of wake effect model.

The wake boundary forms a cone-like shape in Fig.1, and in the wake boundary wind speed decreases with respect to the distance between the adjacent WTs (X). This decreased wind speed trickles down to the lowest, if not all of the WTs under the wake effect. The intensity depends on the location and distance between the adjacent WTs. The closer the WT is from the wake effect source, the greater the wake effect intensity is. Hence, the farther the WT is from the wake effect source, the less the wake effect intensity is. In this situation, it is advisable to introduce the wake effect modeling to determine the appropriate u_i with known ambient wind speed and direction. This aims to determine the extent to which the wake effect may be borne with the minimal power losses and operational cost [21]. Wake effect models are typically classified into kinematic models [22], [23] and field models [24]. Some of the established kinematic models for wake effect modeling include Jensen model, Ainslie model, and Larsen model.

In the Jensen model [23], the wake effect behind the upstream WTs exhibits a linear expansion characteristic. Hence, the wind speed within a wake boundary decreases to the magnitude of the downstream WT velocity, as shown in Fig. 1. In the Ainslie model, a parabolic eddy viscosity model in which the wake turbulence combines with the ambient turbulence wake is developed. Differential equations are formulated and solved to obtain the results. Hence, more time is necessary to obtain a solution. This model is more suitable for the dynamic analysis of WTs. The Larsen model is a semi-analytic wake effect model that considers the wake effect modeling in three scenarios, i. e., non-wake, partial wake, and full wake effects, which is slightly similar to the Jensen model. It is applicable in capturing and analyzing the velocity deficit when the downstream distance exceeds three times the rotor diameter [21]. Among all the wake effect models employed for both onshore and offshore wind farms, the Jensen model is the most widely used because of its simplicity and accuracy in computational analysis [23].

Therefore, the brief mathematical formulations of the Jensen model are outlined below using Fig. 1, which are used as part of the optimization strategy. In the wake effect modeling of wind farm, a WT with different wind speeds and directions is considered. The first scenario is a non-wake effect or the i^{th} WT is outside the wake boundary. This implies that the wind speeds in all WTs are equal, and the wind velocity deficit does not exist under the non-wake effect. u_i is expressed as:

$$u_i = u_o \tag{1}$$

However, in the second scenario, if the i^{th} WT is completely within the boundary of a single full wake effect. u_i is expressed as:

$$u_i = u_o\left(1 - \frac{2a}{1+\alpha\left(X/R_1\right)^2}\right) \tag{2}$$

where a is the axial induction factor; and α is the entrainment constant. The axial induction factor a is typically in the range of 0.2-0.4, and α determines the speed of wake boundary expansion with respect to X [25], [26], is expressed as:

$$\alpha = \frac{0.5}{\ln\left(\dfrac{Z}{Z_o}\right)} \tag{3}$$

where Z is the hub height; and Z_o is the surface roughness length at a certain location, i.e., the height above the ground at which the wind speed is theoretically zero. The length varies depending on the landscape under consideration. For plain terrains, Z_o is 0.3 m and varies with the locations [27].

In the third scenario, a part of the WT rotor blade lies partially within the wake boundary, which is considered as a partial wake effect. In this case, some areas of the WT rotor blades are affected by the wake upstream of the WT. The other areas may experience different forms of the wake effect. Hence, u_i for the partial wake effect is expressed as:

$$u_i = u_o\left(1 - \frac{2a}{1+\alpha\left(X/R_1\right)^2}\right)\frac{A_{T,wake,i}}{A_{T,total,i}} \tag{4}$$

where $A_{T,wake,i}$ is the partial rotor area under wake effect; and $A_{T,total,i}$ is the total rotor area.

In the final scenario, a WT experiences many wake effect forms from the upstream and/or downstream WTs [28]. For instance, by considering many full wake effects (excluding partial wake effect) acting on the i^{th} WT, the resultant u_i is expressed as follows.

$$u_i = u_o\left[1 - \sqrt{\sum_{j=1}^{m_i}\left(1 - \frac{2a}{1+\alpha\left(X/R_1\right)^2}\right)_j^2}\right] \tag{5}$$

where m_i is the number of WTs with wake effect.

Generally, all scenarios of WTs experiencing wake effects at different displacements are considered. The other formulations considered for analytical purposes are as follows.

$$R_d = R_r\sqrt{\frac{1-a}{1-2a}} \tag{6}$$

$$R_1 = \alpha X + R_r \tag{7}$$

$$C_t = 4a(1-a) \tag{8}$$

where R_d is the downstream rotor radius; R_r is the rotor radium; and C_t is the trust coefficient.

In short, the wake effect model leads to the output power loss of 10%-15% [5] or more because the reduced wind speed capture is controlled.

B. Output Power Modeling of Wind Farm

The amount of output power that a WT in a wind farm can extract from the available wind speed depends on many factors. Previously, onshore or offshore wind farms were designed using sparse or simple spacing rules. The WTs were laid along regular power grids. Although this design aids in maintaining the navigational routes of small or medium wind farms, it also has its own problems. Recently, large wind farm designs are square or rectangular and usually have the same WT specifications, as shown in Fig. 2.

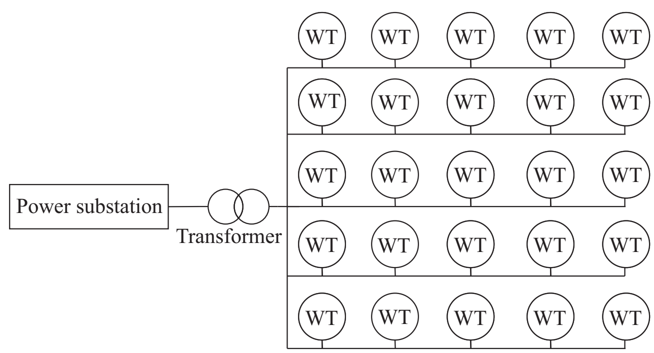

Fig. 2. Diagram of regular wind farm.

In Fig. 2, the generated output power of a WT P_{wt} is calculated as:

$$P_{wt} = \frac{1}{2}C_p\rho A U^3 \tag{9}$$

where C_p is the power coefficient of WT; ρ is the air density; A is the swept area of WT; and U is the general wind speed.

The P_{wt} is proportional to the cube of the wind speed and swept area or the square of the rotor radius. Considering Betz theory [29], the C_p for a commercial WT is 40% [3]. Therefore, P_{wt} is simplified as:

$$P_{wt} = 0.3U^3 \tag{10}$$

Moreover, P_{wt} is regulated according to the available wind speed at a particular time and location. These regulations [16] are guided by the following expression:

$$P_{wt}(U) = \begin{cases} 0 & U < 3\,\text{m/s} \\ 0.3U^3 & 3\,\text{m/s} \le U < 12\,\text{m/s} \\ 518.4\,\text{kW} & 12\,\text{m/s} \le U \le 25\,\text{m/s} \\ 0 & U > 25\,\text{m/s} \end{cases} \tag{11}$$

The foregoing determines the cut-in, cut-out, and rated wind speeds with their corresponding output power for each WT, as shown in Fig. 3.

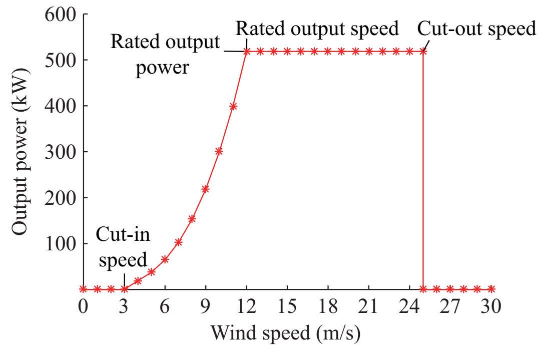

Fig. 3. Output power curve for WT.

In the wind farm, the total ideal output power $P_{wt_{tot,ideal}}$ and total actual output power $P_{wt_{tot,actual}}$ generated by the total number of WTs N_t under wake effect conditions are obtained using the following expressions.

$$P_{wt_{tot,ideal}}=\sum 0.3u_o^3 \quad U=u_o \tag{12}$$

$$P_{wt_{tot,actual}}=\sum 0.3u_i^3 \quad U=u_i \tag{13}$$

Moreover, the total output power of WTs $P_{tot,wts}$ for both the ideal and actual situations (in Fig. 2) with respect to their P_{wt} can be obtained as:

$$P_{tot,wts}=\sum P_{wt} \quad \forall U \tag{14}$$

Finally, the overall annual energy production AEP of the wind farm is calculated as:

$$AEP=8760P_{tot,wts} \tag{15}$$

The expected efficiency η of the wind farm with N_t WTs is expressed as:

$$\eta=\frac{P_{tot,wts}}{N_t P_{wt_{tot,ideal}}} \tag{16}$$

C. Installation Cost (Investment) Modeling

The cost of WTs can be calculated using a function that depends on N_t [9]. This consists of constant and variable terms, which decrease as N_t increases. At any point, an additional WT is equal to a certain fractional cost. Thus, the cost decreases as the purchased volume increases. Therefore, the total installation cost of the entire wind farm per year $Cost$ is calculated as:

$$Cost=N_t\left(\frac{2}{3}+\frac{1}{3}\mathrm{e}^{-0.00174N_t^2}\right) \tag{17}$$

In short, the WT cost and maximum discount are assumed to be 1 and 33.3%, respectively.

D. Optimization of Objective Function

Finally, the objective function for the optimization of WFLO is the energy minimization cost. Therefore, the objective function is the ratio of the total cost of installation to $P_{tot,wts}$ generated by N_t [9].

$$Objective=\min\left(\frac{Cost}{P_{tot,wts}}\right) \tag{18}$$

The foregoing aims to obtain the minimum cost per unit output power produced in a wind farm irrespective of the WT location.

E. Wind Speed Scenario Modeling

The possibility of a preferred wind speed and WT position should be appropriately considered before installation. The rule of thumb stated in [30] indicates the required spacing of WTs within a wind farm. However, wind flows naturally have probabilistic characteristics. They have different speeds, densities, and directions, yet dominant in a particular direction at a given location. At any particular wind speed direction, a WFLO will exhibit a particular arrangement that may or may not generate optimal output power. Considering the probability density function $P_U(\cdot)$, the wind speed follows a particular Weibull distribution as follows.

$$P_U(U,k,c)=\frac{k}{c}\left(\frac{U}{c}\right)^{k-1}\mathrm{e}^{-\left(\frac{U}{c}\right)^k} \quad 0<U<\infty \tag{19}$$

where c is the scale parameter; and k is the shape parameter.

A circular boundary was illustrated in [31] for a predominant wind direction. However, for practicality, a square WFLO of dimension $l\times l$ which is placed diagonally to face the wind speed is considered in this study. This WFLO is further divided into a certain number of cells to represent the possible locations of the WTs, as shown in Fig. 4.

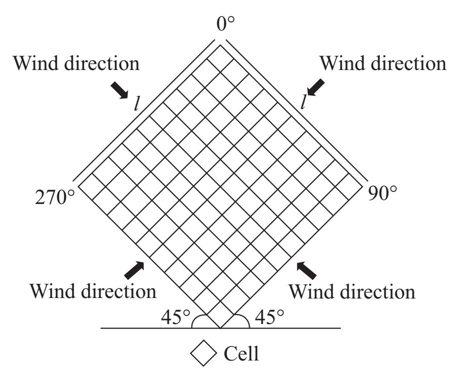

Fig. 4. Wind farm boundary of dimension $l\times l$ and wind directions.

To verify the robustness of the optimization strategy, three study scenarios of wind speeds and directions for the WFLO are chosen. Wind directions are divided into 36 equal intervals (i.e., 10° each interval) from 0° to 350°. Each WT can rotate with the prevailing wind directions.

F. WFLO Constraint Modeling

The appropriate placement of WTs in a given parcel of land to obtain the overall objective of minimizing the losses and operation costs is known as micro-siting. Inadequate micro-siting leads to the poor overall performance and reduced WT lifespan. Nevertheless, the worst problem emanates from changing the WT locations after installation.

In the past, a scattered WFLO is more advantageous for the wind farm owner as this reduces the wake losses. Recently, based on the rule of thumb for regular-shaped WFLO design, the required spacing of WTs is from $8D$ to $12D$ in the main wind flow direction and $3D$ to $5D$ in the crossflow direction, where D is the rotor diameter [32]. This is more evident in regular onshore and offshore wind farms arranged in a site according to traditional layouts, such as irregular shapes and in-line and staggered form.

Considering micro-siting involves uncertainties [33] and many other factors, certain constraints [34] are incorporated in the proposed optimization strategy. The first constraint involves the introduction of the wind farm boundary to ensure that only one WT can be placed within a certain area at a time. The length l and breadth b constraints of a regular WFLO are satisfied as $0 \le x_i \le l$ and $0 \le y_i \le b$, respectively, where x_i and y_i are the transverse and longitudinal variables, respectively. The second constraint regulates the spatial proximity. Thus, there must be sufficient minimal distance within which two WTs can be installed. In the third constraint, all the WTs within the wind farm have the same specifications. These constraints were selected to satisfy the required conditions of the proposed strategy.

III. Proposed Three-step Strategy for WFLO

The proposed three-step strategy for the WFLO consists of the WFLO design, PSO-based optimization, and wake effect modeling using the Jensen model. The three-step strategy algorithm is employed to obtain the optimal location for the WTs and achieve the objective function. The strategy involves a sequential procedure to obtain the objective function, leading to high output power with a reduced wind farm wake effect.

Three case studies are also investigated to ascertain the robustness of the strategy, which include constant wind speed and direction, constant wind speed with variable wind direction, and variable wind speed with variable wind direction, respectively.

The operation function of each block in the diagram is explained in the next subsections.

A. WFLO Design

The WFLO of the square wind farm which is placed diagonally to face the wind direction is proposed. The diagonal of the wind farm lies horizontally on the x axis. This wind farm can be considered as the best layout only when the wind direction is normal to the diagonal axis. This allows the wind farm placed in a diagonal form to have a broader surface area facing the high wind direction and generate optimal output power, as shown in Fig. 4. With the placement of the wind farm in the diagonal form, the distance between adjacent WTs in a cell is the hypotenuse (longer distance). These distance increases when the WTs are perpendicular to the wind directions. Many possible WFLOs were considered, and the proposed approach satisfied all the required strategies. The assumption is only applicable to the situations where many WTs are necessary for the WFLO.

B. PSO-based Optimization

In the proposed WFLO, the PSO ensures the appropriate placement of the WTs to achieve overall optimal power generation. The algorithm shifts the locations of WTs to new locations in each iteration to obtain an updated objective function. This is repeated until all criteria have been satisfied and a suitable location that will lead to the attainment of the objective function is selected.

The procedure begins with the input of the basic parameters of the entire wind farm, including the WT specifications, square wind farm dimension, terrain features, wind scenario, wind speed, wind direction, number of WTs, PSO features (functions and parameters), and Jensen model data. The WFLO is laid at 0° from the north (wind farm boundary at 45° to x axis), assuming that it is the predominant wind direction. A given number of WTs are placed randomly and the initial objective function is calculated. The PSO algorithm is run in MATLAB to obtain the next objective function, which is compared with the previous one and then updated as a new objective function. Finally, upon obtaining a better objective function, the Jensen model verifies the spacing between adjacent WTs. This indicates that the procedure should be repeated until the required result is obtained. The flowchart of PSO for obtaining the proposed WFLO is presented in Fig. 5. In Fig. 5, $Iter$ is the number of iteration; and $Iter_{max}$ is the maximum number of iteration.

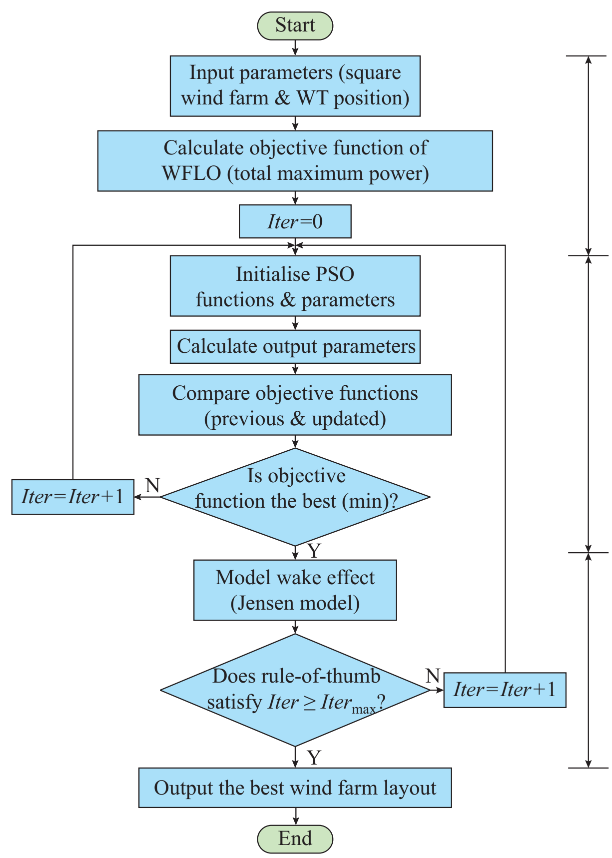

Fig. 5. Flowchart of PSO for WFLO.

C. Wake Effect Modeling Using Jensen Model

The Jensen model verifies and ensures that the spacing between adjacent WTs follows the rule of thumb. In Fig. 4, the distance between two adjacent cells is 200 m. However, with the diagonal placement of wind farms, the distance among the neighboring cells is 282.84 m. This provides wider distances among the WTs, which are two or more cells apart, complying with the rule of thumb [32]. The adjacent wake effects are negligible and accordingly ignored in the formulation because of the wider spacing.

IV. Simulation and Results

In this section, the MATLAB simulation results for the proposed WFLO in the three case scenarios are discussed relative to the wake effect and objective function. The WTs in the wind farm have the same data specifications: $Z=60$ m; $Z_o=0.3$ m; $D=40$ m; trust coefficient $C_t=0.88$; selected total wind farm dimension is 2 km × 2 km. The wind farm dimension is subdivided into 100 possible WT positions or cells (200 m × 200 m). The PSO parameters are used for the quick response; and the particle restriction parameters are inertia weight coefficient $w=0.5$, Acceleration coefficient constants $c_1=2.5$, $c_2=2.5$, and the maximum number of iterations $Iter_{max}=100$. A uniform distribution is applied in selecting random numbers r_1 and r_2 between 0 and 1.

A. Case Study 1: Constant Wind Speed and Direction

In this case, the WFLO is considered under a constant wind speed of 12 m/s at a constant wind direction from the north (0°). After the thorough application of the proposed three-step strategy, the optimized wind farm is illustrated in Fig. 6(a) and is compared with those in [11], [12].

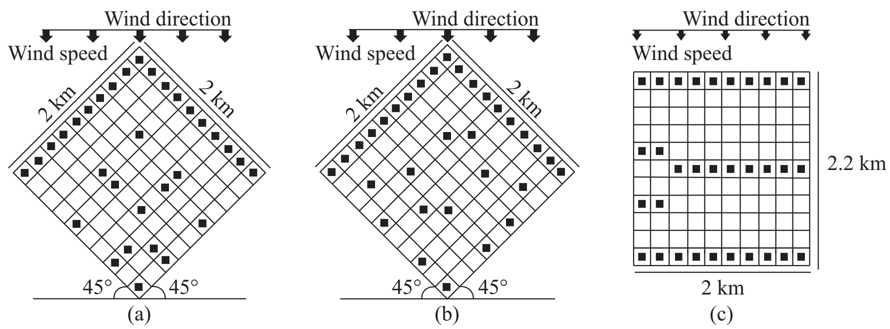

Fig. 6. Results of case study 1. (a) WFLO of the proposed strategy. (b) WFLO of [12]. (c) WFLO of [11].

The distance between adjacent WTs exceeds the minimum requirement of the rule of thumb. Therefore, adjacent WTs are not considered in the formulation because their spacing in the vertical direction is even larger. Hence, the strategy ensures that the wake effect on the downstream WTs is reduced to achieve greater output power. Figure 7 provides the details of the WFLOs with 32 WTs (in Fig. 6).

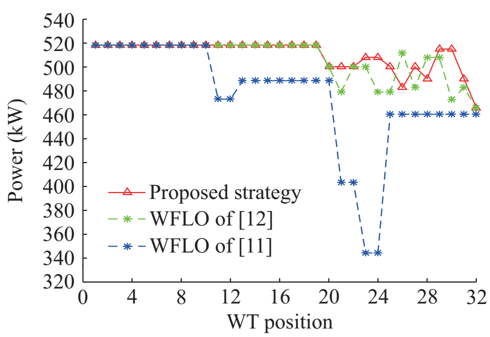

Fig. 7. Output power of WTs at various positions.

In the WFLO of [11], the first 10 WTs generated optimal power; thereafter, the output power of the remaining 22 WTs started to decrease. The least recorded output power in the wind farm was 344.3119 kW. The general performance of the WFLOs is summarized in Table I.

In the case of [12], the reduction in output power started after the first 19 WTs. The rest of the WTs had a marginal wake effect on the downstream WTs. The lowest recorded WT output power was 470.2074 kW. In the proposed WFLO, although the output power reduction started after the first 19 WTs, its resilience remained the same as the remaining 13 WTs. All the WTs recorded significantly high output power except for the last WT with a minimum value of 465.9432 kW.

Considering the objective function of the WFLO, [11] obtained a 91.74% efficiency with an objective function of 0.00155. This was because more than two thirds of the WTs were detrimentally influenced by the wake effect in the boundaries. In the WFLO of [12], 97.77% efficiency was achieved. It also reduced the wake effect to obtain an objective function of 0.001537 because of the improved GA optimization algorithm. As for the proposed WFLO using the three-step strategy, further improvements were observed: 98.42% efficiency was achieved, and the objective function was further reduced to 0.00142. Although the 13 WTs were exposed to the wake effect in the WFLO, this effect was minimal compared with that on the other WTs. Figure 8 de-

TABLE I
PERFORMANCE OF CASE STUDY 1

Optimization strategy	N_t	Total power (kW)	Wake loss (kW)	*AEP* (MWh)	*Objective*	Efficiency (%)
Proposed strategy	32	16326.59	262.20	143020.98	0.00140	98.42
WFLO of [12]	32	16251.56	337.24	142363.67	0.00154	97.77
WFLO of [11]	32	15218.20	1370.60	133311.42	0.00155	91.74

picts the minimization of the objective function for the proposed strategy and those for [11], [12].

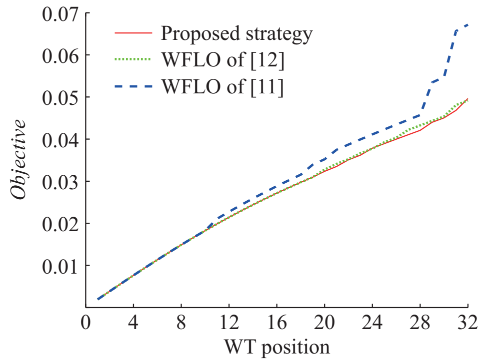

Fig. 8. Comparison of optimized objective functions of WFLO.

The proposed optimized wind farm shown in Fig. 6(a) achieved significant power generation. Hence, with the further minimization of the objective function, the average efficiency was 98.42% of the expected ideal output power.

B. Case Study 2: Constant Wind Speed and Variable Wind Direction

In this case, a scenario where the wind speed is constant with variable wind direction is considered. A 12 m/s mean wind speed with equal probabilities of blowing from all directions is considered. All the WTs are located within the wind farm and have the ability to rotate according to the variable wind direction. At any angle of the wind direction, the WFLO also has different layout patterns corresponding to the wind speed. With the proposed strategy, the algorithm quickly solved all the instances for one wind direction. However, as more wind directions were introduced, some instances were not optimally solved. After a considerable number of iterations, a solution was obtained, and the optimal WFLO generated higher output power. This aided in further minimizing the objective function using the proposed strategy. The optimal WFLO is compared with those in [9], [21] and is depicted in Fig. 9(a). The general performances of the WFLO summarized in Table II are compared with those in [9], [21].

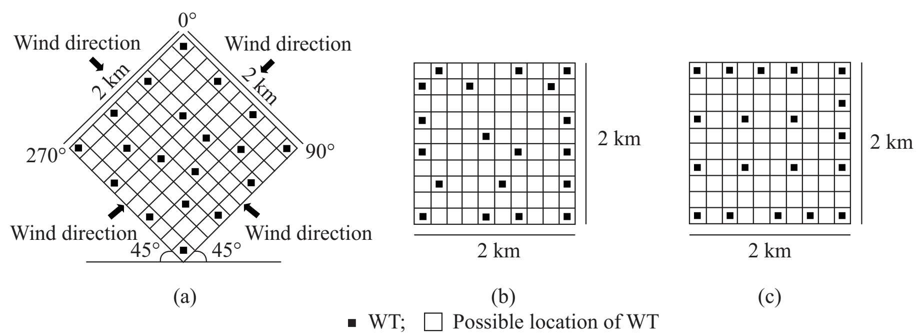

Fig. 9. Results of case study 2. (a) WFLO of the proposed study. (b) WFLO of [9]. (c) WFLO of [21].

TABLE II
PERFORMANCE OF CASE STUDY 2

Optimization strategy	N_t	Total power (kW)	Wake loss (kW)	*AEP* (MWh)	*Objective*	Efficiency (%)
Proposed strategy	19	9741.30	108.30	85333.79	0.00164	98.90
WFLO of [21]	19	9549.00	300.60	83649.24	0.00168	96.95
WFLO of [9]	19	9244.70	604.90	80983.57	0.00174	93.86

In [9] and [21], more wake effects were observed because most of the WTs were aligned with some of the wind directions. In some cases, more than four WTs were aligned. Most of the WTs were close to the wind farm boundary. However, in employing the three-step strategy, high output power was recorded. This was because of the reduced wake effect caused by the uniformly distributed WTs. As a result, the objective function was reduced to 0.00164 with an efficiency of 98.90%.

C. Case Study 3: Variable Wind Speed and Direction

For this case study, variable wind speed and wind direction are considered similar to those in [9], [35]. High wind speeds are predominant between 270° and 350°. This case study is practically the same as case study 2. The mean wind speeds of 8, 12 and 17 m/s are used one after the other from the predominant wind directions, as shown in Fig. 10(a).

As shown in Fig. 10, in the WFLOs of [9] and [35], most of the WTs are laid along the wind farm boundaries. Some were crowded and detrimentally influenced by the wake effect, especially those aligned with the wind speed.

The proposed strategy in this case study had a well-laid uniform WFLO that considered the possibility of wind blowing from any direction. As a result, the wake effect was reduced to obtain an optimal WFLO with a high efficiency of 98.9022%. Based on the summary in Table III, the three-step strategy is able to overcome most of the problems reported in other existing studies with the same constraints [9], [11], [12], [35]. Hence, this demonstrates that the output power and efficiency are further improved, thus minimizing the objective function.

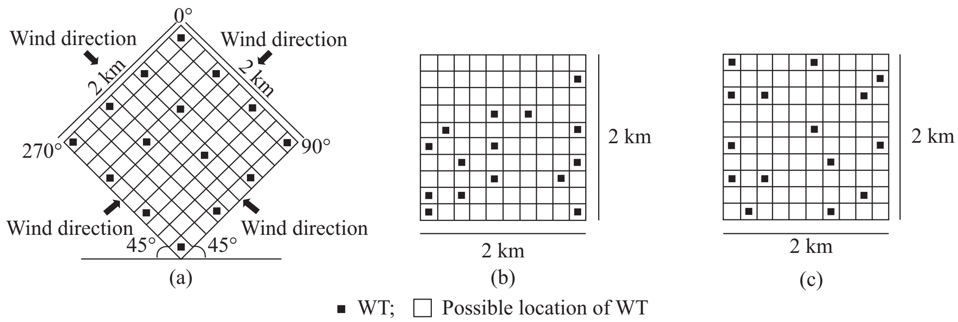

Fig. 10. Results of case study 3. (a) WFLO of the proposed strategy. (b) WFLO of [35]. (c) WFLO of [9].

TABLE III
PERFORMANCE OF CASE STUDY 3

Optimization strategy	N_t	Total power (kW)	Wake loss (kW)	*AEP* (MWh)	*Objective*	Efficiency (%)
Proposed strategy	15	15020.78	166.72	131582.03	0.000891	98.90
WFLO of [35]	15	1470.00	13717.50	12877.20	0.000910	97.16
WFLO of [9]	15	13460.00	1727.50	117909.60	0.000994	94.62

V. CONCLUSION

In this paper, a three-step strategy for minimizing the objective function of the WFLO is introduced. The first step involves the diagonal design of the $2\,\text{km}\times 2\,\text{km}$ wind farm where a broader surface area is exposed to the wind. In the second step, the PSO algorithm is applied to find the optimal positions for each WT and utilize all the possible wind speeds while satisfying the necessary spacing between adjacent WTs. Finally, based on the rule of thumb, the Jensen model was considered to investigate and ascertain the wake effects acting on the WTs at all positions. The optimized WFLOs under the three case studies of wind speeds and directions were analyzed. Accordingly, the position of each WT was appropriately selected to obtain possible higher output power.

With the use of the three-step strategy, the simulated results for the objective function were further minimized in the WFLO for all instances. Compared with the results of other existing studies, $P_{tot,wts}$ and η were significantly improved. Through the use of the proposed strategy, the losses as well as the wear and tear were reduced, allowing the WT to attain the expected lifespan as a result of the wake effect minimization. Finally, if operationalized, the strategy is anticipated to provide quick investment returns with higher installation efficiencies. This demonstrates that a better WFLO can be achieved using the proposed three-step strategy.

REFERENCES

[1] A. N. Nichenametla, S. Nandipati, and A. L. Waghmare, "Optimizing life cycle cost of wind turbine blades using predictive analytics in effective maintenance planning," in *Proceedings of Reliability and Maintainability Symposium (RAMS)*, Orlando, USA, Jan. 2017, pp. 1-6.

[2] P. Hou, J. S. Zhu, K. Ma *et al*., "A review of offshore wind farm layout optimization and electrical system design methods," *Journal of Modern Power Systems and Clean Energy*, vol. 7, no. 5, pp. 975-986, Jul. 2019.

[3] F. Cheng, L. Qu, and W. Qiao, "Fault prognosis and remaining useful life prediction of wind turbine gearboxes using current signal analysis," *IEEE Transactions on Sustainable Energy*, vol. 9, no. 1, pp. 157-167, Jun. 2017.

[4] Y. Y. Chen, Z. Y. Dong, K. Meng *et al*., "A novel technique for the optimal design of offshore wind farm electrical layout," *Journal of Modern Power Systems and Clean Energy*, vol. 1, no. 3, pp. 258-263, Dec. 2013.

[5] R. J. Barthelmie, G. C. Larsen, and S. T. Frandsen, "Comparison of wake model simulations with offshore wind turbine wake profiles measured by sodar," *Journal of Atmospheric and Oceanic Technology*, vol. 23, no. 7, pp. 888-901, Jul. 2006.

[6] R. Shakoor, M. Y. Hassan, A. Raheem *et al*., "Wind farm layout optimization using area dimensions and definite point selection techniques," *Renewable Energy*, vol. 88, pp. 154-163, Apr. 2016.

[7] K. Chen, M. X. Song, X. Zhang *et al*., "Wind turbine layout optimization with multiple hub height wind turbines using greedy algorithm," *Renewable Energy*, vol. 96, pp. 676-686, Oct. 2016.

[8] L. Wang, M. E. Cholette, Y. Fu *et al*., "Combined optimization of continuous wind turbine placement and variable hub height," *Journal of Wind Engineering & Industrial Aerodynamics*, vol. 180, pp. 136-147, Sept. 2018.

[9] G. Mosetti, C. Poloni, and B. Diviacco, "Optimization of wind turbine positioning in large windfarms by means of a genetic algorithm," *Journal of Wind Engineering and Industrial Aerodynamics*, vol. 51, pp. 105-116, Jan. 1994.

[10] S. A. Grady, M. Y. Hussaini, and M. M. Abdullah, "Placement of wind turbines using genetic algorithm," *Renewable Energy*, vol. 30, pp. 259-270, Feb. 2005.

[11] A. Mittal, "Optimization of the layout of large wind farms using genetic algorithm," Ph. D. Dissertation, Case Western Reserve University, Ohio, USA, May 2010.

[12] R. Shakoor, M. Y. Hassan, A. Raheem *et al*., "The modelling of wind farm layout optimization for the reduction of wake losses," *Indian Journal of Science and Technology*, vol. 8, no. 17, pp. 1-9, Aug. 2015.

[13] J. Patel, V. Savsani, V. Patel *et al*., "Layout optimization of a wind farm using geometric pattern-based approach," *Energy Procedia*, vol. 158, pp. 940-946, Feb. 2019.

[14] J. C. Bansal and P. Farswan, "Wind farm layout using biogeography based optimization," *Renewable Energy*, vol. 107, pp. 386-402, Jul. 2017.

[15] P. Hou, W. Hu, M. Soltani *et al*., "Combined optimization for offshore wind turbine micro siting," *Applied Energy*, vol. 189, pp. 271-282, Mar. 2017.

[16] O. Abedinia, A. Ghasemi, and N. Ojaroudi, "Improved time varying inertia weight PSO for solved economic load dispatch with subsidies and wind power effects," *Complexity*, vol. 1, no. 4, pp. 40-49, Oct. 2014.

[17] P. Hou, W. Hu, C. Soltani *et al*., "Offshore wind farm layout design considering optimised power dispatched strategy," *IEEE Transactions on Sustainable Energy*, vol. 8, no. 2, pp. 638-647, Apr. 2017.

[18] C. P. Ajit, C. John, J. Lars *et al.*, "Offshore wind farm layout optimization using particle swarm optimization," *Journal of Ocean Engineering and Marine Energy*, vol. 4, pp. 73-88, Jan. 2018.

[19] K. Veeramachaneni, M. Wagner, U. M. O'Reilly *et al.*, "Optimizing energy output and layout costs for large wind farms using particle swarm optimization," in *Proceedings of 2012 IEEE Congress on Evolutionary Computation (CEC)*, Brisbane, Australia, Jun, 2012, pp. 1-7.

[20] P. Hou, W. Hu, C. Chen *et al.*, "Optimization of offshore wind farm layout in restricted zones," *Energies*, vol. 113, pp. 487-496, Oct. 2016.

[21] S. D. O. Turner , D. A. Romero, P. Y. Zhang *et al.*, "A new mathematical programming approach to optimize wind farm layouts," *Renewable Energy*, vol. 63, pp. 674-680, Mar. 2014.

[22] H. Kim, K. Kim, C. Bottasso *et al.*, "Wind turbine wake characterization for improvement of the Ainslie eddy viscosity wake model," *Energies*, vol. 11, no. 10, pp. 1-19, Oct. 2018.

[23] S. A. Mir-Hassani and A. Yarahmadi, "Wind farm layout optimization under uncertainty," *Renewable Energy*, vol. 107, pp. 288-297, Jul. 2017.

[24] Z. Yang and Y. Li, "Individual pitch control for wind turbine load reduction including wake interaction," in *Proceedings of the 2011 American Control Conference (ACC)*, San Francisco, USA, Jun.-Jul. 2011, pp. 5207-5212.

[25] H. Liang, L. Zuo, J. Li *et al.*, "A wind turbine control method based on Jensen model," in *Proceedings of 2016 International Conference on Smart Grid and Clean Energy Technologies (ICSGCE)*, Chengdu, China, Oct. 19-22, 2016, pp. 207-211.

[26] P. Luzzatto-Fegiz. (2020, Jul.). "A one-parameter model for turbine wakes from the entrainment hypothesis," *Journal of Physics: Conference Series*.[Online]. doi: 10.1088/1742-6596/1037/7/072019.

[27] D. Petkovic, S. H. Ab Hamid, Z. Cojbasic *et al*., "Adapting project management method and ANFIS strategy for variables selection and analyzing wind turbine wake effect," *Natural Hazards,* vol. 74, no. 2, pp. 463-475, Jun. 2014.

[28] R. Shakoor, M. Y. Hassan, A. Raheem *et al*., "Wake effect modeling: a review of wind farm layout optimization using Jensen's model," *Renewable and Sustainable Energy Reviews*, vol. 58, pp. 1048-1059, May 2016.

[29] Y. Moumouni and N. Galupa, "Experimental evaluation of a wind turbine's energy dependency on air density," in *Proceedings of 2018 Advances in Science and Engineering Technology International Conferences (ASET)*, Abu Dhabi, UAE, Feb. 2018, pp. 1-4.

[30] G. Rong. (2020, Jul.). "How much land is needed for wind turbines," [Online]. Available: https://sciencing.com

[31] A. Kusiak and Z. Song, "Design of wind farm layout for maximum wind energy capture," *Renewable Energy*, vol. 35, no. 3, pp. 685-694, Mar. 2010.

[32] M. R. Patel, "Wind and solar power systems: design, analysis, and operation," 2nd ed., Boca Raton, USA: CRC Press, 2005.

[33] S. Tahari, M. Shafie-khah, and G. J. Osorio, "Stochastic modelling of renewable energy sources from operators' point-of-view: a survey," *Renewable and Sustainable Energy Reviews*, vol. 81, no. 2, pp. 1953-1965, Jan. 2018.

[34] M. Wagner, J. Day, and F. Neumann, "A fast and effective local search algorithm for optimizing the placement of wind turbines," *Renewable Energy*, vol. 51, pp. 64-70, Mar. 2013.

[35] R. Shakoor, M. Y. Hassan, A. Raheem *et al.*, "The modelling of wind farm layout optimization for the reduction of wake losses," *Indian Journal of Science and Technology*, vol 8, no. 17, pp. 1-9, Aug. 2015.

Philip Asaah received the Higher National Diploma (HND) from Sunyani Polytechnic, Ghana, 2006, in electrical and electronic engineering. He has been working in Ghana Broadcasting Corporation as a Technician Engineer since 2009 to date. Currently, he is pursuing the M.S. degree in Nanjing Tech University, Nanjing, China. His research interests include wind/solar power generation, smart grid and control science.

Lili Hao received the B.S. degree and M.S. degree from Hohai University, Nanjing, China, in 2001 and 2004, and the Ph.D. degree from Southeast University, Nanjing, China, in 2010, all in electrical engineering. She was a Visiting Scholar in the School of Electrical Engineering and Computer Science, Washington State University, Pullman, USA, from 2015 to 2016. Since 2012, she has been an Associate Professor at Nanjing Tech University, Nanjing, China. Her current research interests include power system security and reliability.

Jing Ji received the B.S. degree from Nanjing Tech University, Nanjing, China, in 2017, where she is currently working toward the M.S. degree. Her current research interests include wind power generation and smart grid systems.